

Electrothermal Microactuators Based On Dielectric Loss Heating

Bizhan Rashidian and Mark G. Allen
 School of Electrical Engineering
 Microelectronics Research Center
 Georgia Institute of Technology
 Atlanta, GA 30332-0250

ABSTRACT

In this paper a new method for microactuation, based on excitation using the heat generated as a result of dielectric loss of materials at high frequencies, is presented. We have realized this concept by fabricating electrothermal microactuators, composed of a layer of the copolymer of vinylidene fluoride and trifluoroethylene (PVDF-TrFE), on top of polyimide, using a fully integrated, self aligned process. These actuators show larger deflection per unit temperature rise than conventional resistively heated electrothermal microactuators due to the properties of the materials used. In addition, they are easy to fabricate, can be remotely excited and are capable of underwater operation. The actuation mechanism has been verified and a simplified model as well as a finite element model have been developed. The measured values are in good agreement with those predicted by the model.

INTRODUCTION

Several types of electrothermal microactuators, using heat as the source of microactuation, have been reported [1-9]. These include shape memory alloys, pneumatic structures, and electrothermal bimorphs, which are a generalization of conventional bimetals. In this paper we focus on the last type, the electrothermal bimorphs. In general, electrothermal microactuators can generate large deflections and relatively large forces, have relatively good scaling properties, and usually require small input voltages. The thermal energy which is the source of excitation is usually provided through the heat dissipated in a resistor. However, this additional resistor may make the fabrication more complicated, degrade the mechanical performance of the device or increase the thermal time constant of the device. Also the thermal conductivity and the thickness of the materials used is usually high, which increases the thermal loss of the device. As a result usually high input currents are usually needed to provide the temperature rise necessary for the operation of the device. The resultant high temperature rise makes it difficult to operate these devices in liquid environments such as water or human blood.

In this paper we introduce a new concept for microactuation based on the heat generated as a result of dielectric loss of materials at high frequencies. With this approach instead of using the heat generated by an additional resistive heater, the heat generated as a result of dielectric loss of the actuator material at RF frequencies is the excitation source. As a result, the additional heating element, with its associated disadvantages, can be eliminated since the heating element is integral to the actuator itself. These actuators require lower drive voltages and currents than the resistively heated ones, and are capable of being remotely excited through inductive coupling of input signal, with no direct physical contact to the input source. We have also taken advantage of

using polymers to demonstrate this idea which allows two further advantages to be exploited: the relatively low thermal conductance of polymers insulates the actuator, thus keeping the heat concentrated in the actuator itself, which reduces the thermal loss and as a result the input power required; and the large flexibility and high yield strain of the polymers, which allows large deflections even with temperature rises of a few °C. The polymer we have used as the heating element is PVDF-TrFE. We have reported its use as an integrated piezoelectric material previously [10].

CONCEPT

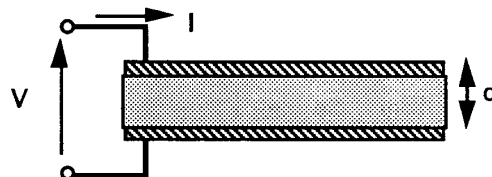


Figure 1. A capacitor with lossy dielectric

The basic idea of RF heating is shown in Figure 1. An RF signal, $V(t)$, is applied to a parallel plate capacitor with a lossy dielectric. The heat generated in the dielectric is given by:

$$\frac{P_{th}}{Vol.} = \frac{1}{2} \omega \epsilon_r'' \epsilon_0 |E_0|^2 \quad (1)$$

Here the left hand side of the equation is the thermal power generated per unit volume, ω is the radian excitation frequency, ϵ_r'' is the imaginary part of the relative permittivity, ϵ_0 is the permittivity of free space, and E_0 is the electric field across the dielectric, which is related to the applied voltage and the plate separation d . Examination of equation (1) shows that the generated heat should increase as the square of the applied electric field. Since ϵ_r'' may also be a function of frequency, the dependence of (1) on frequency must be determined for each material system.

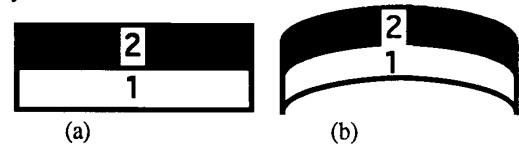


Figure 2. Basic bimorph structure.

Figure 2-a shows the basic bimorph structure. The two layers have different coefficients of thermal expansion. When the structure is heated, the top layer tends to expand more than the bottom one, and as a result the structure bends up as shown

in Figure 2-b. If the lossy material shown in Figure 1 is used as one of the layers of Figure 2, the structure can be actuated without the need for any additional heating element.

In order to actually realize the above concept, suitable materials should first be chosen. The materials for the two layers should have large difference in the coefficient of thermal expansion, relatively close yield strains, low thermal conductivities, and should be compatible with micromachining processes. One of the layers should also have high enough dielectric loss at RF frequencies to provide the temperature rise needed to achieve the desired deflection.

Based on the above requirements, PVDF-TrFE, as the heating layer, and DuPont PI2611D polyimide as the second layer, were chosen. Some properties of these materials are given in Table 1. For comparison, corresponding values for some other combinations of materials used in previously reported bimorphs is also reported. The difference in the coefficient of thermal expansion for PVDF-TrFE and PI2611D is between one to two orders of magnitude larger than the other materials.

TABLE 1

Some Properties of Some Materials used for Electrothermal Bimorphs

Material	Coefficient of Thermal Expansion [10 ⁻⁶ /°C]	Young's Modulus [GPa]
PVDF-TrFE	140	2.3
PI 2611D	3	8.3
Al	23	69
Au	14.3	80
Si	2.6	162
SiO ₂	0.4	74

In order to measure the dielectric loss of PVDF-TrFE, a parallel-plate capacitor similar to the one shown in Figure 1 consisting of the film sandwiched between two evaporated aluminum electrodes was fabricated on a silicon wafer. This capacitor was then analyzed using an HP8753B network analyzer to determine the imaginary and real parts of the dielectric constant. Assuming no resistive losses are present, the phase of the input admittance Y is given by:

$$\angle Y = 90^\circ - \tan^{-1}(\epsilon''/\epsilon') \quad (2)$$

Here ϵ' and ϵ'' represent the real and imaginary part of the permittivity of the material, respectively. If the material were lossless, the phase would remain constant at 90 degrees over the frequency range. The deviation from 90 degree phase represents the dielectric loss of the material. Figure 3 shows the result of measurement. The bold horizontal line in this figure shows the 90° phase, which would be the result of measurement, if the material were lossless. As can be seen, the loss factor of this material is significant.

A second test was performed to verify actual heat generation from this material prior to microstructure fabrication. Due to the low thermal capacity of the film, and

the low temperature rise, direct measurement of temperature was not practical; so infrared thermometry was used for this measurement. Figure 4 shows the experiment that was performed.

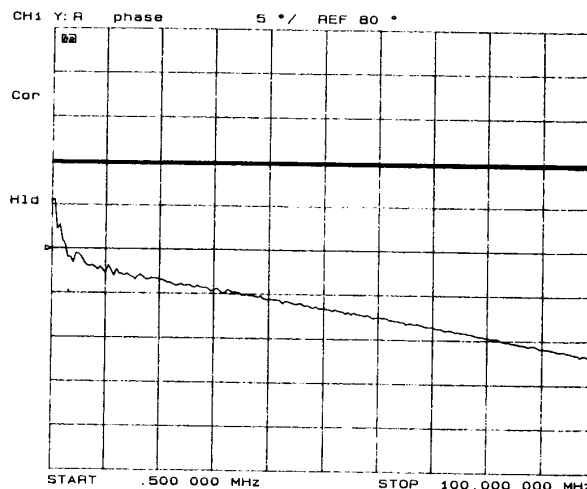


Figure 3: Dielectric loss of PVDF-TrFE versus frequency. The horizontal axis begins at a frequency of 0.5 MHz and ends at 100 MHz. The vertical axis begins at a phase angle of 55° and ends at 105°. The boldface horizontal line is at a constant phase of 90° which, corresponds to a lossless dielectric.

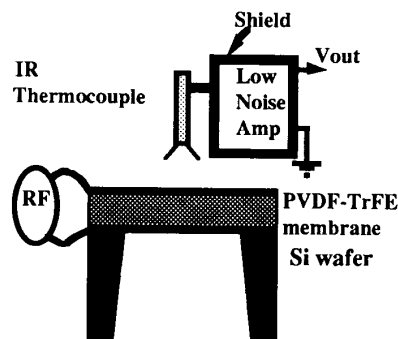


Figure 4. Measuring the temperature rise of the material

A released membrane of PVDF-TrFE was fabricated by spin casting a solution of PVDF-TrFE in N,N-dimethylacetamide (DMAC) on top of a 2" Si wafer and isotropically etching it from the backside. This sample was excited by an RF source. The IR radiation of the material (P_r) is proportional to its temperature (T) as given by:

$$P_r = \sigma T^4 \quad (3)$$

Here σ is the emissivity of the surface of the device. An IR thermocouple (IR t/c-J-140-3, Exergen Co.) was used as the IR detector. The sensitivity of this detector was 46 $\mu\text{V}/^\circ\text{F}$. The output signal of this detector was amplified using a shielded low noise amplifier. This signal is proportional to the

temperature rise of the material. Figure 5 shows the result of the measurement.

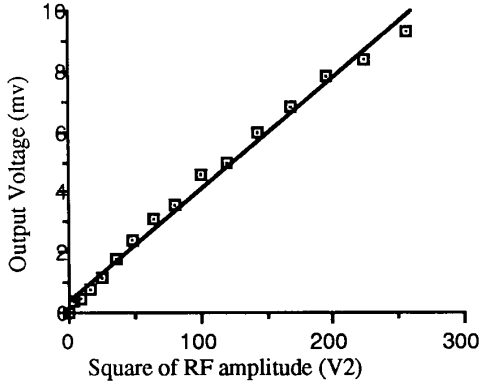


Figure 5. The results of IR thermometry

As expected from equation (1), the temperature rise is proportional to the input electrical power, which is in turn proportional to the square of the amplitude of the applied signal. As it is seen the measurement is in good agreement with the expected theoretical value. Taking into account the gain of the amplifier (40), and the sensitivity of IR detector, it is found out that the temperature rise is several °C for the range of applied voltages.

Once the feasibility of the device had been experimentally verified, microactuator design and fabrication was undertaken. In order to design the structures, bimetal theory was utilized.

SIMPLE BIMETAL THEORY

The basic bimetal structure has been analyzed by Timoshenko [11]. Using the assumptions of static equilibrium and the continuity of strain at the interface between the materials, the radius of curvature (r) is found to be:

$$r = \frac{2}{3} \frac{\frac{7}{4}(t_1 + t_2)^2 - 2t_1t_2 + \frac{E_1 b_1 t_1^3}{E_2 b_2 t_2} + \frac{E_2 b_2 t_2^3}{E_1 b_1 t_1}}{\Delta\alpha \Delta T (t_1 + t_2)} \quad (4)$$

where t , E , and b represent thickness, Young's moduli and width, respectively, and indices 1 and 2 refer to layers 1 and 2, respectively. Using simple geometry, the deflection d for a bimetallic cantilever beam of length l is found to be:

$$d = l^2 / 2r \quad (5)$$

and for a simply supported bridge of length l (neglecting residual stress), the deflection is found to be:

$$d = l^2 / 8r \quad (6)$$

Timoshenko [11] has found the force resulting from the deflection of the beam, by finding the external force necessary to keep the tip at zero deflection:

$$R = \frac{9}{48} \frac{EWh^2}{l} \Delta\alpha\Delta T \quad (7)$$

Here R , E , W , h and l represent the force at the tip of the beam, Young's modulus, the width, the thickness and the length of the beam, respectively. $\Delta\alpha$ and ΔT represent the difference in the coefficient of thermal expansion and the temperature rise of the beam, respectively.

The above model has the following implicit assumptions: uniformity of temperature across the beam, temperature independence of material properties, negligible friction at the interface of the layers, pure bending of the beam (linear distribution of strain across the beam), neglecting the effect of boundaries on the distribution of stress across the beam, one dimensional analysis and small deflections.

Important practical points obtained from this model are that the output deflection is proportional to the square of the length of the beam, inversely proportional to its thickness, and proportional to both the mismatch in the coefficient of thermal expansion between the two materials and to the temperature rise. It can be verified that for maximum deflection, it is best to have the thicknesses of both layers equal. The force is proportional to Young's modulus of the beam, its width, and the square of its thickness, and is inversely proportional to its length.

FABRICATION

The fabrication sequence is shown in Figure 5.

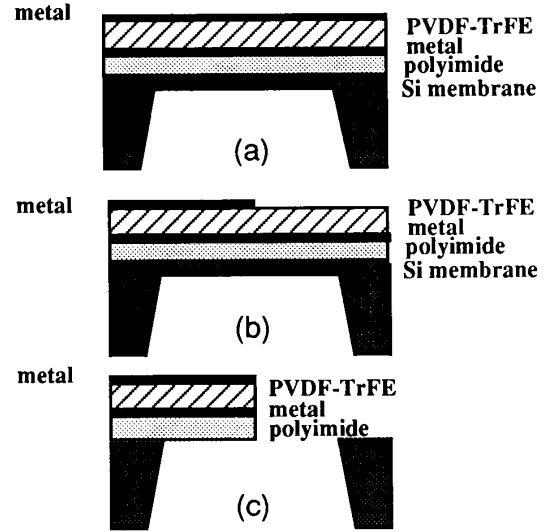


Figure 5. The fabrication sequence for a cantilever beam: a) The stack of polyimide, metal, PVDF-TrFE, and metal on top of Si membrane. b) The structure after patterning the top layer. c) The released structure

Starting from a p+ doped, anisotropically (KOH) etched Si membrane in a (100) silicon wafer, a layer of

PI2611D is spin cast at 2500 rpm for 90 seconds, baked at 120 °C for 10 minutes, and cured at 350 °C for 1 hour. A layer of titanium (2000 Å) is deposited using DC sputtering. The PVDF-TrFE is then spin-cast from solution in DMAC at 3000 rpm for 25 seconds. This film is soft baked at 95 °C for 15 minutes and hard baked at 140 °C for 15 minutes. A layer of aluminum (2500 Å) is then evaporated. This top Al layer is patterned using standard photolithography and wet etched in a PAN (phosphoric-acetic-nitric acid) etching solution. The structure is then plasma etched from the top in 95%/5% O₂/CF₄ plasma. The plasma etches through all of the layers and the silicon membrane in all areas which are not protected by the top aluminum layer, making the process fully self-aligned. Upon completion of the plasma etch, the structures have been released. The thin Si left underneath the structures can optionally be removed by etching the structure from the backside in 5%/95% O₂/CF₄ plasma. Contacts were then made to the two metallized layers. Figure 6 shows a photograph of some of the actual devices.

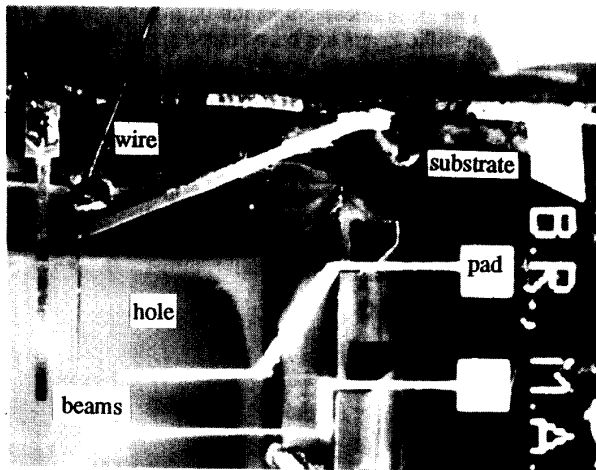


Figure 6: A photograph of some fabricated devices. Note the hole etched into the substrate over which the cantilever beams are suspended.

TESTING AND RESULTS

Several released bridges and cantilever beam structures have been fabricated using the above process, ranging in length from tens of microns to a few millimeters. The structures were tested by applying 0-16 volt peak RF signal with frequencies from 1 MHz up to 100 MHz and observing the resultant deflection. The deflection was a function of both frequency and amplitude of the applied signal. Deflections exceeding 250 μm at 3 volts and 900 μm at 16 volts for cantilever beams have been observed. Figure 7 shows the deflection of the central part of a bridge versus the square of the amplitude of the applied signal.

As expected the deflection should be proportional to the temperature rise, which is proportional to the applied RF power, which is in turn proportional to the square of RF amplitude. As can be seen, the measurement agrees qualitatively with the functional form of the theory, although contributions due to residual stresses in the bridge may have to be taken into account in order to achieve quantitative agreement. Figure 8 shows the deflection of the bridge versus frequency, again as expected deflection increases with the increase in frequency.

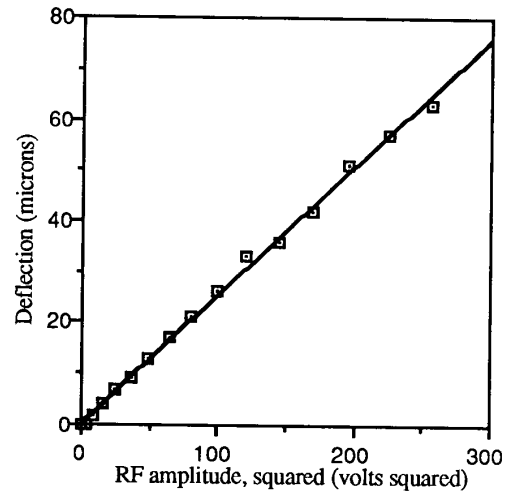


Figure 7: The dependence of deflection of the center of the bridge to the RF amplitude. The frequency of the RF signal was held constant at 4 MHz. The width of the bridge is 300 μm, the thickness of each layer is 4 μm, and the length of the bridge is 5000 μm.

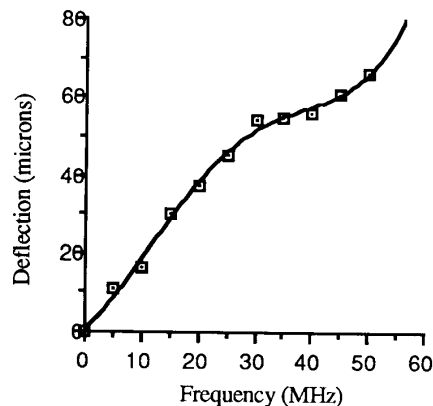


Figure 8: The dependence of deflection of the center of the bridge on the input frequency. The size of the bridge is identical to that measured in Figure 7. The magnitude of the input signal was held constant at 16 volts.

The actuation speed is limited by the thermal, and not the mechanical, time constant of the structure. We have observed mechanical response of these devices to pulsed (gated) input signals at gating frequencies of up to 50 Hz.

These devices have also been successfully tested under water. In this experiment the structure was immersed in a petri dish filled with DI water and the deflection was observed with microscope while the signal was applied.

In order to remotely excite these structures, a wire wound inductor was connected to the input of the beam, another inductor, connected to the output of an RF source at 11 MHz, was brought close to it. By gating the RF source the structure was successfully actuated.

ANALYTICAL AND F.E.M. MODELING

A simplified model, taking into account the convective and conductive heat transfer from the device to ambient has been developed, using piece wise linear, one dimensional approximation for the temperature profiles. Figure 9 shows the basic approach.

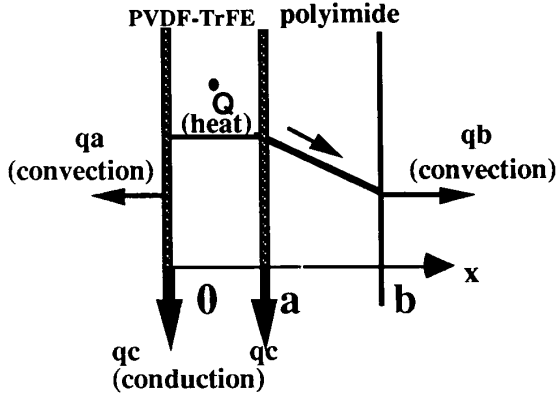


Figure 9: Simplified heat transfer model, cross section of the beam is shown. The cross hatched regions represent metal contacts, the left and right hand sides are at ambient temperature (T_{am}).

Using an energy balance approach along with the heat transfer equations, we find the temperatures in PVDF-TrFE and polyimide layers as:

$$T(0) = \frac{\dot{Q} - T_{am} \left[\frac{hA}{1+f} - 2hA - 2 \frac{K_{Al} W t_{Al}}{L} \right]}{hA \left[\frac{2f+1}{1+f} + 2 \frac{K_{Al} W t_{Al}}{L} \right]}$$

$$T(b) = \frac{fT(0) + T_{am}}{1+f}$$

Where $T(0)$ and $T(b)$ are the temperatures at $x=0$ and $x=b$, respectively. T_{am} represents ambient temperature, h is the convective heat transfer coefficient, A is the top surface area of the beam, W and L are the beam width and length and t_{Al} and K_{Al} represent the thickness and the conductivity of the metallic layer, respectively. f is given by:

$$f = \frac{k}{h(b-a)}$$

Here k is the thermal conductivity of polyimide and $(b-a)$ is its thickness. The parameter " f " is a dimensionless quantity, representing the ratio of the heat transferred through conduction across polyimide to that transferred from the surface area of polyimide to ambient through convection. Physically, the presence of $(b-a)$ in the denominator of " f " is due to the fact that thermal conductivity is a diffusion process, and depends on the slope of the temperature profile. If " f " were small one would expect the high thermal resistivity of

polyimide compared to that resulting from convective heat transfer to the ambient, and as a result a large temperature drop across polyimide. However, due to the small value of the thickness of polyimide used in the devices considered here, and despite its low thermal conductivity, by plugging in typical values for the thickness of polyimide ($4 \mu\text{m}$), its thermal conductivity (about $0.15 \text{ W}/(\text{m} \cdot \text{K})$, assuming that of PI2555) and the value of h (about $5-50 \text{ W}/(\text{m}^2 \cdot \text{K})$ in air) it is found that " f " is very large (about 10^3 to 10^4); as a result the temperature across the polyimide is quite uniform. Plotting the temperature profile predicted from the model has shown uniform distribution of temperature across the polyimide and PVDF-TrFE layers.

Another important point is shown in Figure 10. Here the temperature rise is shown versus the coefficient of convective heat transfer of the ambient (h). As it is seen the temperature rise is very sensitive to the value of h .

It should be mentioned that in the above model, for heat conduction along the beam to the substrate (which is assumed to be at the ambient temperature) only the conduction through the metallic layers has been considered. It has also been assumed that both metallic layers have the same thermal conductivities. These assumptions are valid for the devices considered here, however, due to one dimensionality of the model, one can easily take into account the other components of conductive heat transfer by plugging in an effective value for K_{Al} , incorporating the thermal conductivity of other layers.

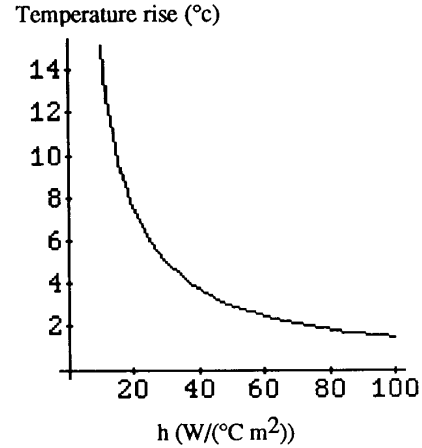


Figure 10: The predicted dependence of temperature rise of the beam on the convective heat transfer coefficient.

Figure 11 shows the plot of output deflection, resulting from finite element analysis of a 1mm long, $2 \mu\text{m}$ thick cantilever beam, versus the temperature rise. The analysis has been done using the ANSYS program with one dimensional elements and 300 nodes. The results of the F.E.M. model are in good agreement to the analytical model, based on Timoshenko's work, for small deflection, but deviate as the deflection gets larger. The same nonlinear behavior has been observed in the actual cantilever beams as well. Figure 12 shows the result of measurements on a 3mm long, $8 \mu\text{m}$ thick, $240 \mu\text{m}$ wide cantilever beam in large deflection.

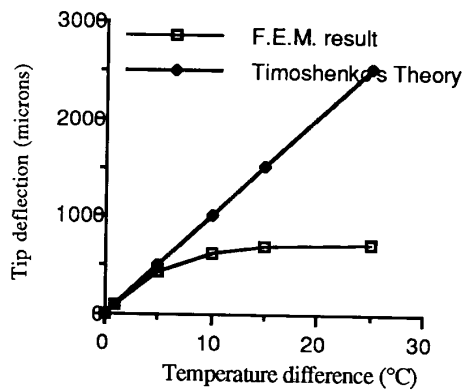


Figure 11: The result of F.E.M. simulation compared with that based on Timoshenko's theory.

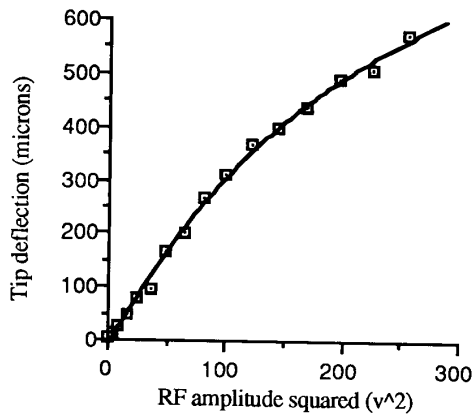


Figure 12: The nonlinear behavior observed in a cantilever beam, 3000 microns long, 240 microns wide and 8 microns thick with RF excitation frequency of 30 MHz.

The microactuators discussed above can deflect vertically (i.e., perpendicular to the substrate surface). In order to achieve full three-dimensional actuation, lateral actuators (i.e., in the plane of the substrate surface) are also required. Lateral actuators have been achieved with this material system by using a modified fabrication sequence to place the polyimide and PVDF-TrFE layers side-by-side instead of on top of each other. These fully integrated lateral microactuators have also been successfully tested.

CONCLUSIONS

A new concept of microactuation using RF heating has been presented. This concept has been demonstrated by fabricating cantilever beams and bridges using PVDF-TrFE/polyimide bimorphs. The heating mechanism has been verified and a simplified model as well as a finite element model have been developed. Measurements are in good agreement with the model and show superior performance of these structures over conventional resistively heated structures. Using 1 mW input RF power, with several °C rise in the temperature, we have observed deflections exceeding 700 μm from 3000 mm long, 240 μm wide 8 μm thick cantilever

beam. Comparing this to 90 μm reported in [1] for a resistively heated bimorphs of 500 μm long, 4 mm thick, excited by 200 mW with several hundred °C rise in temperature, about two orders of magnitude in deflection performance is achieved. The presented structure can also work under water and be excited by remote RF power, which gives it the potential for biomedical application and making free to move microrobots.

ACKNOWLEDGMENT

Microfabrication was carried out in the Georgia Tech Microelectronics Research Center. The donation of PVDF-TrFE powders used in this work by Atochem Corporation, as well as the donation of polyimide by DuPont, is gratefully acknowledged. The authors would also like to thank Mr. Chong H. Ahn, Mr. Young W. Kim and Mr. Bruno Frazier of Georgia Tech for valuable technical discussions.

REFERENCES

- [1] W. Riethmuller and W. Benecke, "Thermally Excited Silicon Microactuators," IEEE Trans. Elec. Dev. Vol. 35, June 1988 pp758-763.
- [2] J. H. Jerman, "Electrically-Activated Micromachined Diaphragm Valves," Technical Digest IEEE Solid-State Sensor and Actuator Workshop, Hilton Head, pp. 65-69, 1990.
- [3] D. Moser, O. Brand and H. Baltes, "A CMOS Compatible Thermally Excited Silicon Oxide Beam Resonator With Aluminum Mirror," IEEE Transducers-International Solid-State Sensors and Actuators, pp. 547-550, 1991.
- [4] M. Parameswaran, Lj. Ristic, K. Chau, A. M. Robinson and W. Allegretto, "CMOS Electrothermal Microactuators," IEEE Micro Electro Mechanical Systems Workshop, pp. 128-131, 1990.
- [5] J. W. Judy, T. Tamagawa, and D. L. Polla, "Surface Micromachined Linear Thermal Microactuator," Proc. IEEE Int. Electron Devices Meeting, pp26.5.1- 26.5.4, 1990.
- [6] N. Takeshima and H. Fujita, "Polyimide Bimorph Actuators for a Ciliary Motion System," Proc. ASME, DSC-Vol.32, pp. 203-209, 1991.
- [7] J. Ji, L. J. Chaney, M. Kaviani, P. L. Bergstrom, and K. D. Wise, "Microactuation Based on Thermally-Driven Phase-Change," IEEE Transducers-Inter. Solid-State Sensors and Actuators, pp. 1037-1040, 1991.
- [8] C. Doring, T. Grauer, J. Marek, H. P. Trah and M. Willmann, "Micromachined Thermo-electrically Driven Cantilever Structures for Fluid Jet Deflection," Proc. IEEE Micro Electro Mechanical Systems, Feb. 1992, pp.12-18.
- [9] F. C. M. Van De Pol, H. T. G. Van Lintel, M. Elenspoek and J. H. J. Fluitman, "A Thermopneumatic Micropump Based on Micro-engineering Techniques," Sensors and Actuators, A21_23 pp 198-202 1990.
- [10] B. Rashidian and M. G. Allen, "Integrated Piezoelectric Polymers for Microsensing and Microactuation Applications," Proc. ASME, DSC-VOL.32, 1991, pp171-179.
- [11] S. P. Timoshenko, "Analysis of Bi-Metal Thermostats," J. Optical Soc. Amer., vol. 11, pp. 233-255. 1925.